ISSN : 0974 - 7540 Volume 2 Issue 2

Trade Science Inc.

Research & Reviews On Electrochemistry

Full Paper

RREC, 2(2), 2010 [61-68]

Electrochemical behaviours of two carbon steels in a sulfuric acid solution after tensile plastic deformation

Patrice Berthod

Institut Jean Lamour (UMR 7198), Department of Chemistry and Physics of Solids and Surfaces, Faculty of Sciences and Technology, B.P. 70239, 54506 Vandoeuvre-lès-Nancy, (FRANCE)

E-mail : Patrice.Berthod@lcsm.uhp-nancy.fr

Received: 30th April, 2010 ; Accepted: 10th May, 2010

ABSTRACT

A ferritic steel and a ferrito-pearlitic one were subjected to different amounts of tensile strain deformation. Electrodes were prepared from more or less deformed tensile samples, after cutting favouring each of the two studied orientations versus the traction axis. For each of them a cyclic polarisation run was performed between the cathodic domain and the solvent wall in the anodic side. The behaviour in the active state was characterized using the beginning of the potential-increasing part of the curves, with determination of the corrosion potential and current according to the Tafel method. The other part of the curve was used to specify the conditions of passivation and the behaviour in the passive state. Results show that both the amount of plastic strain and the orientation versus the deformation direction influence the electrochemical behaviour of the steels. For example, corrosion current is higher if the plastic strain amount is higher and if the considered surface is perpendicular to axis.

© 2010 Trade Science Inc. - INDIA

KEYWORDS

Carbon steels;
Plastic deformation;
Corrosion;
Sulphuric solution;
Electrochemical measurements.

INTRODUCTION

Cold or hot working of metallic alloys usually deforms significantly their microstructures. These modified structures, which can be easily revealed by metallographic observations can be characterized by a preferential microstructure orientation and the presence of phases obviously deformed. In the last tens of years, it has been shown that such microstructure deformations may lead to changes for several properties of the alloys, notably in the mechanical field[1,2]. Indeed, modifications of mechanical resistance or hardness may occur in steels alloyed or not, in alloys based on aluminium, on copper, ... and for plastic deformation in different modes[3-5]. In addition the new properties may present a marked anisotropy, consequence of the orientation of these preliminary deformations. Plastic deformation can also modify the corrosion behaviour of the alloys, notably of steels alloyed or not, with ferritic, austenitic or martensitic matrix[6-9].

The aim of this work is to examine, in the specific case of two not alloyed steels, one ferritic and one ferrito-pearlitic, the consequences of several plastic deformations performed with different amplitudes, on

the corrosion behaviours of these steels in an acid solution.

EXPERIMENTAL

The two studied steels of the study and their different strained states

Two steels available as bars were initially heat treated (austenitization for 45 minutes at 860°C then air-cooled). Depending on the initial carbon content, one was practically wholly ferritic and the other was ferrito-pearlitic since it contained about 0.48% of carbon (weight percent). They were machined in order to obtain samples for mechanical tensile tests, the heads of which were cylindrical (diameter 12mm x length 50mm) and the main part of which were cylindrical too, with a diameter and a length equal to 7mm and 52mm respectively. They were strained using a MTS QT/100 traction machine, the cell of which has a 100kN capacity. For the two steels, the ruptured samples were cut in different locations for obtaining parts not deformed (heads), homogeneously deformed (main part, far from the rupture surface), or with especially high deformation (very close to the ruptured surface). In the specific case of the ferrito-pearlitic steel, a supplementary tensile test was performed with interruption of the plastic deformation before the appearance of striction, as is to say when the plastic deformation was still homogeneous. Thus, in addition to the zones of striction, only one plastically strained state was obtained for the ferritic steel while two different plastically strained states were obtained for the ferrito-pearlitic steel ("Strained1" and "Strained2", respectively corresponding to 10% and 17% of plastic deformation). Cutting for obtaining the samples needed by the study was performed in order to have, for each strained state (striction zones excepted), a sample for an electrode with a surface parallel to the tensile stress axis (i.e. to the tensile sample axis) and an electrode with a surface perpendicular to this axis.

Preparation of the electrodes and realization of the electrochemical tests

Mounted samples were prepared for both electrochemical experiments and preliminary metallographic examination of their microstructures. The cut samples were connected to a copper wire covered by plastic for electrically isolating from the electrolyte, then embedded in a cold resin+hardener mixture. They were then polished with grinding papers from 240-grit to 1200-grit, ultrasonic cleaned and polished until mirror state and etched with Nital4 (ethanol + 4% HNO_3). In this state the mounted samples were subjected to metallographic examination, using optical microscope equipped with a digital camera (microscope Olympus Vanox-T, camera Olympus DP-11).

Thereafter they were polished with 600-grit paper again, to obtain the surface state needed by the electrochemical measurements. These ones were performed in an aqueous acid solution (H_2SO_4 1N) contained in a cell where the working electrode (steel sample), a reference electrode (Saturated Calomel Electrode: +241.5mV / Normal Hydrogen Electrode) and a counter electrode (graphite) were immersed. The three electrodes were connected to a potensiostat / galvanostat apparatus (Princeton Applied Research, model 263A) driven by the software M352 of EGG/ Princeton. The electrochemical runs were all cyclic polarizations performed at 10mV/s between E_{ocp} – 250mV and 1.9V (E_{ocp} or E(I=0): Open Circuit Potential, which can be assumed to be the corrosion potential).

RESULTS AND DISCUSSION

Microstructures of the samples

The microstructures of the steels, in the not strained state and in the strained states, are illustrated for the two orientations by optical micrographs, in Figure 1 for the ferritic steel and in Figure 2 for the ferrito-pearlitic one. The ferritic steel essentially contains ferritic (Centred Cubic) grains, either isotropic (not strained part and surface perpendicular to tensile axis in the strained part) or elongated (strained part, cross sections parallel to axis). The ferrito-pearlitic steel contains ferrite grains (white) and pearlitic (grey) zones, with the same trend of isotropy or anisotropy for respectively the not strained state and the two strained states. Thus, the tensile deformation induced geometric modifications for the phases present in the microstructures of these two steels (more visible when both ferrite and pearlite are present together in the steel).

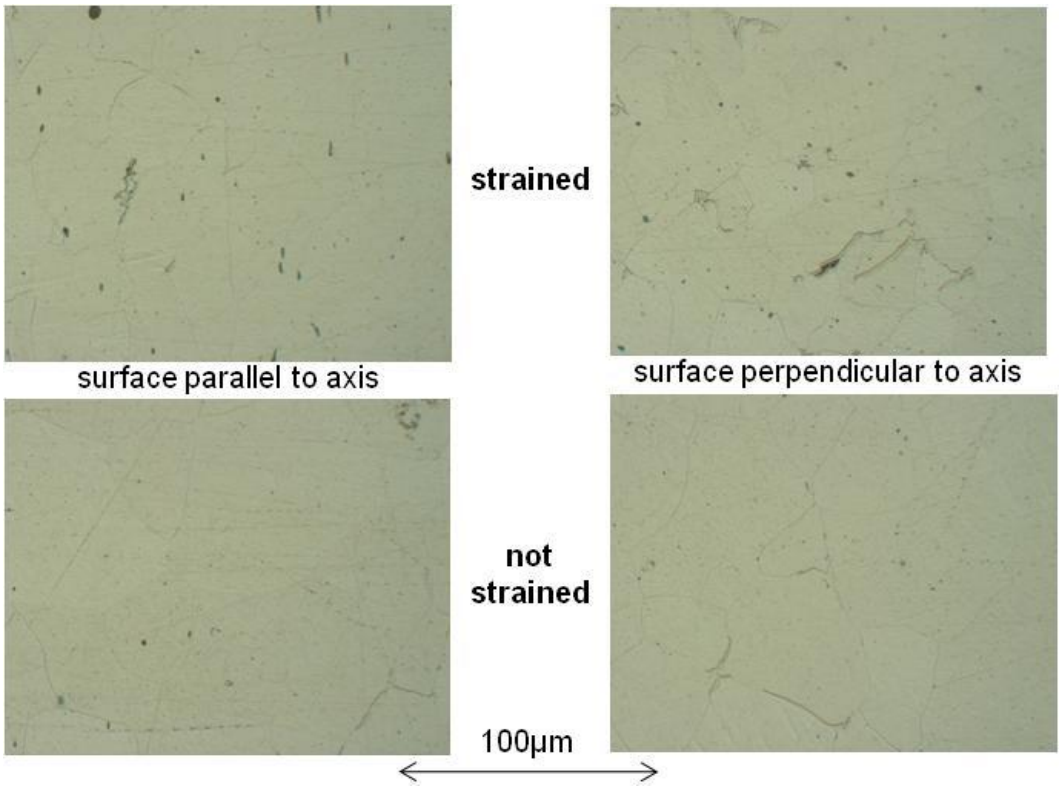

Figure 1 : Ferritic steel - microstructures in the not strained state (bottom) and in the homogeneously strained state (top) for the orientations parallel (left) or perpendicular (right) to the strain direction

Electrochemical tests: corrosion behaviour in the active state

When immersed in the acid solution and without applied potential, the two steels are logically in the active state. The polarization curves performed thereafter can be used first to get information about the behaviour of the steels, versus the strain amount and the surface orientation, when they are still in the active state. Indeed the part between E_{ocp} – 250mV and E_{ocp} + 250mV in the potential-increasing part of the polarization curve can be analyzed using the Tafel method. This one gave the results presented in TABLE 1 (ferritic steel) and TABLE 2 (ferrito-pearlitic steel): values of potential and current density of corrosion E_{corr} and I_{corr} (coordinates of the intersection points of the cathodic and anodic Tafel's straight lines), and of the cathodic and anodic Tafel's coefficients (β_c and β_a).

In all cases the global position of the corrosion potentials, between -0.44V / NHE and 0V / NHE and the not very low corrosion density of currents (order of magnitude of 100µA/cm² to 1mA/cm²), both indicate that all steel electrodes are effectively in the active state, what is not surprising for not-alloyed steels in a sulphuric solution with pH ≈ 0. The cathodic and anodic reactions are then simply $2.H^+ + 2.e \rightarrow H_2$ and $Fe \rightarrow Fe^{2+} + 2e$, as confirmed by the average values of the Tafel coefficients (β_a and β_c respectively near 60 mV / decade (the most often) and 120 mV/ decade). However there is a trend for higher values of the two cathodic Tafel's coefficients when the strained state of the sample is more severe, and especially for the perpendicular orientation.

Concerning the corrosion potentials and corrosion current densities, in the case of the ferritic steel, the values of E_{corr} are a little variable but without any direct relation to the strained state, while, on the contrary, the value of I_{corr} rapidly increases with the deformation, especially for the perpendicular orientation for which the milli-Ampere per cm² is reached.

The same comments can be done concerning the ferrito-pearlitic steel. However the increase in corrosion current with the plastic strain is faster since it is more than doubled between the not strained state and the "Strained2" state. In the zone of striction more than 3mA/cm² is reached, while it was 2mA/cm² for the ferritic steel.

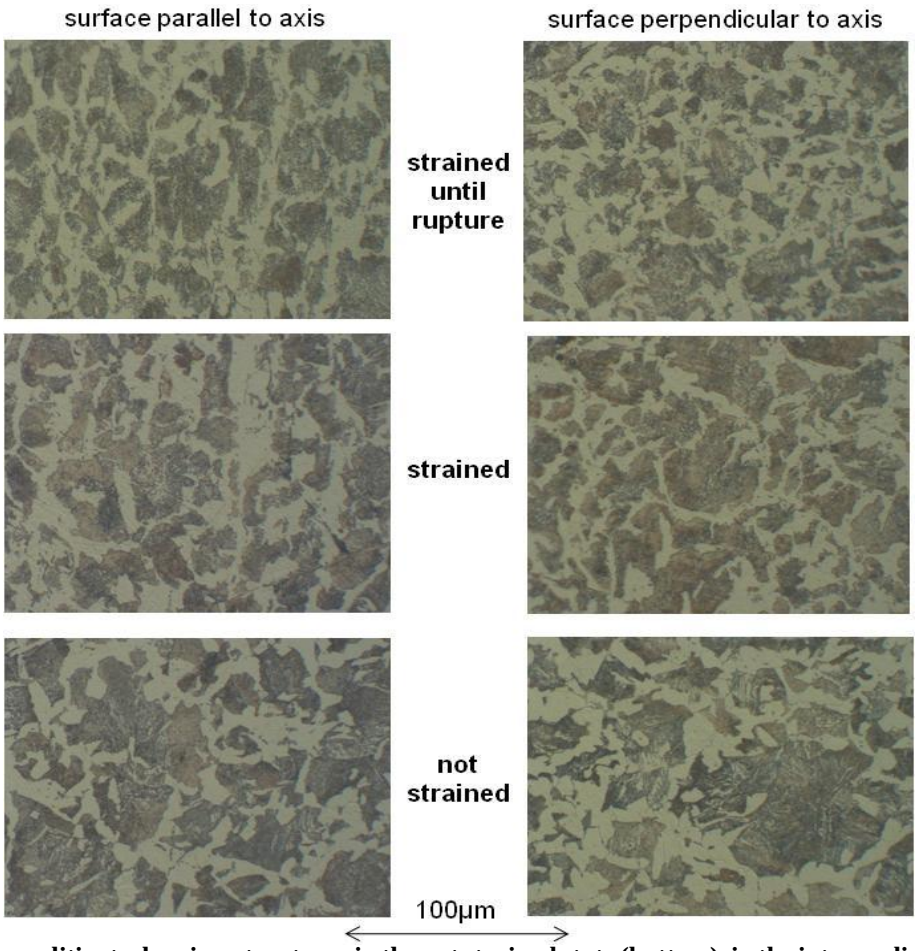

Figure 2 : Ferrito-pearlitic steel - microstructures in the not strained state (bottom), in the intermediate homogeneously strained state (middle) and in the ultimate homogeneously strained state (top) for the orientations parallel (left) or perpendicular (right) to the strain direction

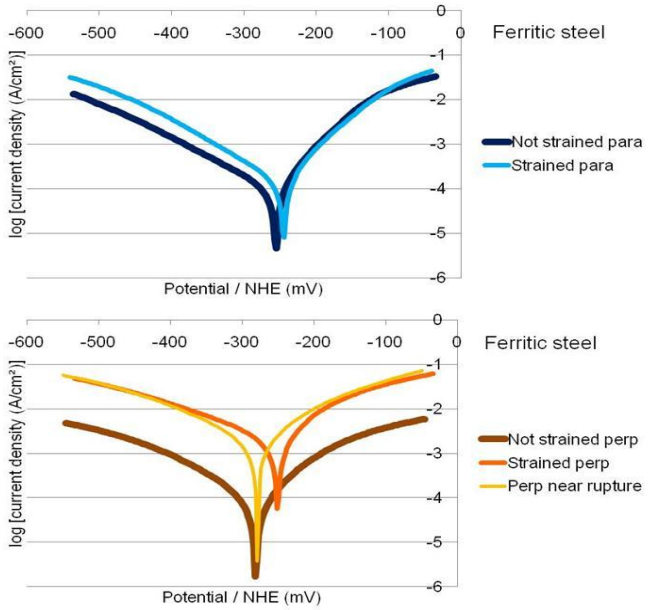

Figure 3 : Ferritic steel - [E_{ocp} -250mV ; E_{ocp} +250mV] sections of the polarization curves (potential-increasing part) used for Tafel calculations

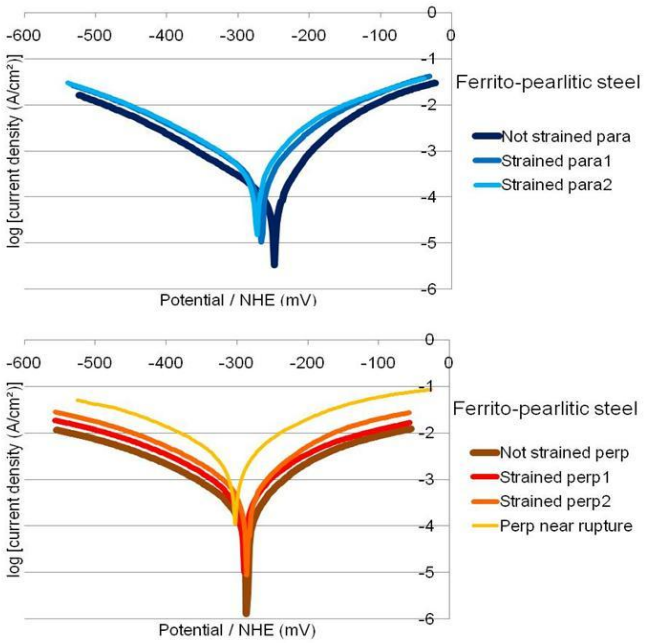

Figure 4 : Ferrito-pearlitic steel - [E_{ocp} -250mV ; E_{ocp} +250mV] sections of the polarization curves (potential-increasing part) used for Tafel calculations

TABLE 1 : Ferritic steel - values of the results obtained by applying the Tafel method to the [E_{ocp} – 250mV; E_{ocp} + 250mV] parts of the E-increasing parts of the polarization curves

FERRITIC STEEL	Surface parallel To deformation axis		Surface perpendicular to deformation axis	
	E_{corr} / NHE (mV)	I_{corr} (mA/cm²)	E_{corr} / NHE (mV)	I_{corr} (mA/cm²)
	β_a (mV / decade)	β_c (mV / decade)	β_a (mV / decade)	β_c (mV / decade)
Not strained	–256	0.101	–281	0.06
	61	126	65	80
Strained	–245	0.153	–251	1.94
	63	114	78	171
Near rupture	Not applicable		–279	1.95
			136	162

TABLE 2 : Ferrito-pearlitic steel - values of the results obtained by applying the Tafel method to the [E_{ocp} – 250mV; E_{ocp} + 250mV] parts of the E-increasing parts of the polarization curves

FERRITO-PEARL. STEEL	Surface parallel to deformation axis		Surface perpendicular to deformation axis	
	E_{corr} / NHE (mV)	I_{corr} (mA/cm²)	E_{corr} / NHE (mV)	I_{corr} (mA/cm²)
	β_a (mV / decade)	β_c (mV / decade)	β_a (mV / decade)	β_c (mV / decade)
Not strained	–249	0.111	–287	0.346
	54	114	111	143
Strained1	–268	0.325	–290	0.611
	73	124	113	147
Strained2	–274	0.424	–286	0.859
	73	128	115	149
Near rupture	Not applicable		–303	3.38
			121	158

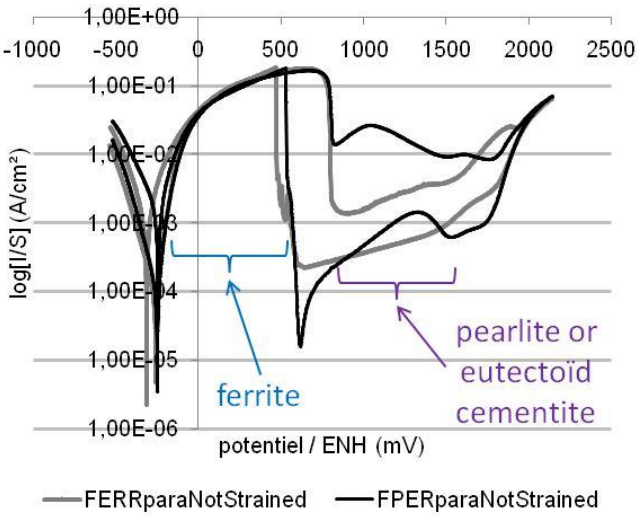

Figure 5 : Superposition of the two cyclic polarization curves obtained for the same state (not strained) and the same orientation (parallel) for the ferritic steel ("FERR") and the ferrito-pearlitic steel ("FPER")

Electrochemical tests: corrosion behaviour in the passive state

Passivation was always possible, but for applied potentials higher than E_{ocp} + 250mV. The whole polarization curves were then considered in order to characterize the conditions of passivation (potentials at which passivation occurs: E_{pass}, maximal density of anodic current before passivation, named critical passivation current: I_{cp}), the anodic current just after passivation (I_{pass}), and the parameters describing the stability of the passive state when the applied potential decreases ($E_{passloss}$).

The global shape of the polarization curves depends on the concerned steel (Figure 5). Indeed, if only one anodic peak can be seen for the ferritic steel, there are two peaks for the ferrito-pearlitic steel: the first one between E_{corr} and about +800mV / NHE (i.e. as the sole one for the ferritic steel) and the second one over the range +800 → +1400 mV / NHE.

Several E-increasing parts of selected polarization curves are displayed as example in Figure 6 for the ferritic steel and Figure 7 for the ferrito-pearlitic one, while some values of potential and of density of current characterizing the E-increasing part and the E-decreasing part of the cyclic polarization curves are given in TABLE 3 for the ferritic steel and TABLE 4 for the ferrito-pearlitic one.

The passage of the two steels from the active state to the passive state is obviously more difficult for the surfaces perpendicular to sample axis than for the surfaces parallel to this axis (the anodic peak is prolonged to higher potentials values). A more strained state, which progressively lowers the passivation potential, tends to facilitate the passivation (Figure 6 and Figure 7).

This can be also seen with the values of passivation potential in TABLE 3 and TABLE 4 (the first one for the ferrite-pearlitic steel, corresponding to passivation of ferrite (1)). However the contrary trend seems to be shown by the increase in critical passivation densities of current, even if I_{cp} does not really clearly depend on the strained state. Nevertheless the anodic current in the passive state, I_{pass}, seems decreasing when the steel (essentially the ferrite-pearlitic one) is more strained. But this can be also induced by the fact that the passivation occurred at lower potentials. Concerning the loss

Full Paper

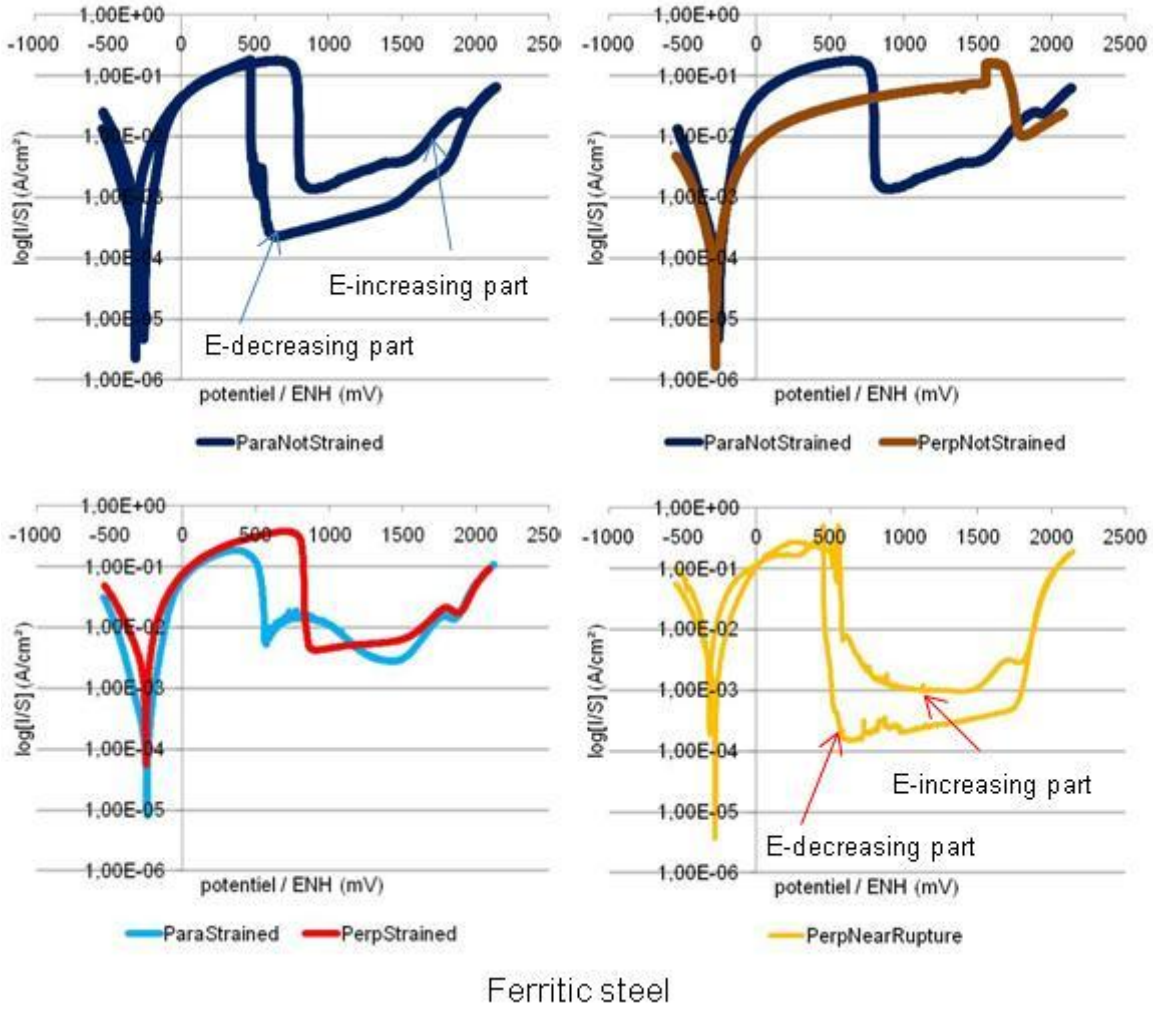

Figure 6 : Ferritic steel - comparison of the potential-increasing parts of the cyclic polarization curves between the two orientations for the not-strained state (top right) and for the homogeneously strained state (bottom left); top left and bottom right: the whole cyclic polarization curves for the surface parallel to axis for the not-strained state, and for the surface perpendicular to the axis close to the rupture zone, respectively

TABLE 3 : Ferritic steel - values of potential and density of current characterizing the achievement of the passive state when the applied potential increases, and its stability when the applied potential decreases

FERRITIC STEEL	Surface parallel to deformation axis			Surface perpendicular to deformation axis		
	I_{cp} (mA/cm²)	E_{pass} / NHE (mV)	I_{pass} (mA/cm²)	I_{cp} (mA/cm²)	E_{pass} / NHE (mV)	I_{pass} (mA/cm²)
	$E_{passloss}$ / NHE (mV)			$E_{passloss}$ / NHE (mV)		
Not strained	178	+799 +477	↑ 1.41 to 3.78	162	+1739 +521	/
Strained	185	+550 +490	5.65	377	+829 +509	↑ 4.31 to 6.25
Near rupture	Not applicable			271	+573 +459	1.00

of passive state when the applied potential decreases, no clear dependence on the strained state or on the orientation can be noted.

General commentaries

Thus several differences of corrosion behaviour in the acid solution of the study were noted between the not deformed zone and the more or less deformed zones. The observations are quite clear concerning the active state (increase in corrosion rate when plastic deformation increases) and consistent with previous results concerning different types of steels[6-9]. Additional information is given in the present study since one also noted an effect of the orientation of the surface with regards to the deformation direction: faster corrosion for the perpendicular orientation. Earlier works showed that such a dependence on the strained state was not

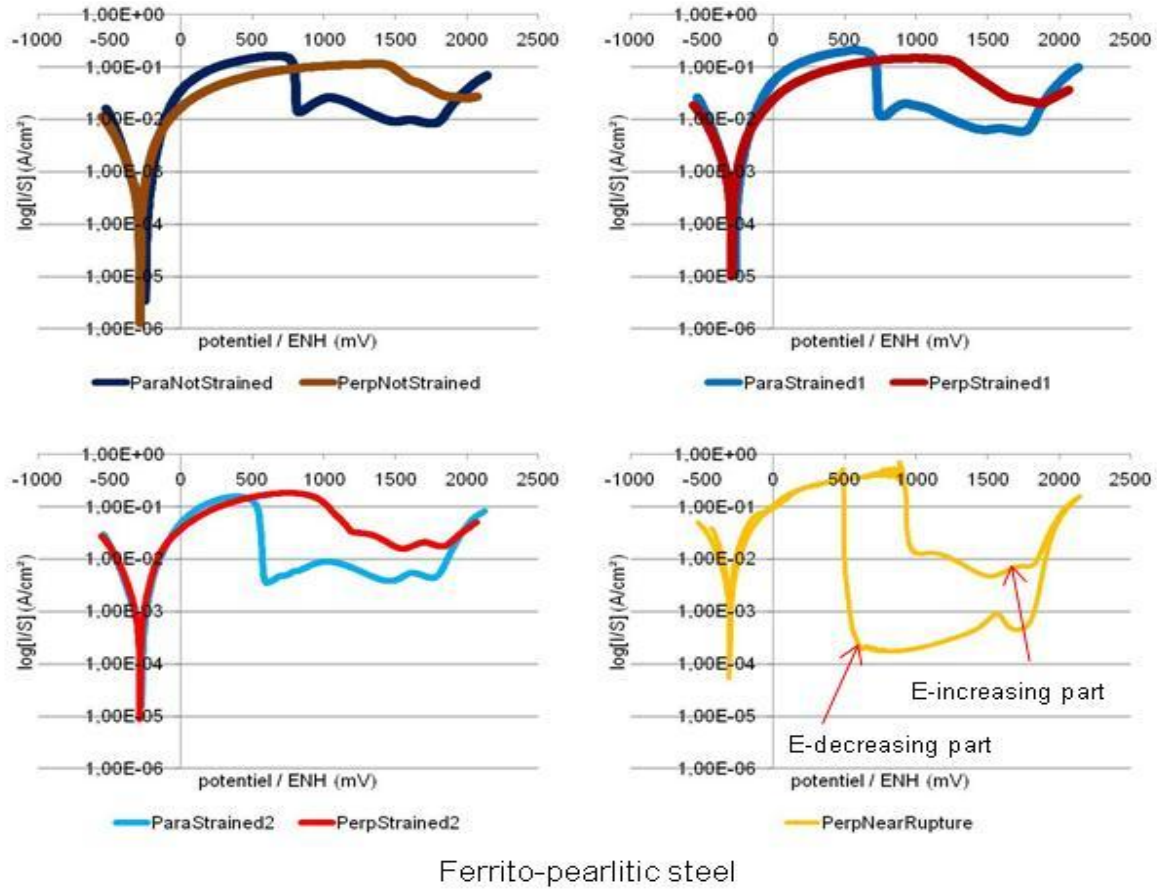

Figure 7 : Ferrito-pearlitic steel - comparison of the potential-increasing parts of the cyclic polarization curves between the two orientations for the not-strained state and the two homogeneously strained states (bottom right: the whole cyclic polarization curve for the surface perpendicular to the axis and close to the rupture zone)

TABLE 4 : Ferrito-pearlitic steel - values of potential and density of current characterizing the achievement of the passive state when the applied potential increases and its stability when the applied potential decreases

FERRITO-PEARLITIC STEEL	Surface parallel To deformation axis			Surface perpendicular to deformation axis		
	I_{cp} (mA/cm²)	E_{pass}/NHE (mV)	I_{pass} (mA/cm²)	I_{cp} (mA/cm²)	E_{pass}/NHE (mV)	I_{pass} (mA/cm²)
	$E_{passloss}$ / NHE (mV)			$E_{passloss}$ / NHE (mV)		
Not strained	165 (1) 26.1 (2)	+803 (1) ↑ +1053 to +1511 (2)	9.13	112	↑ +1450 to +1922 +484	25.3
	↓ +1529 to +1327 (2), +535 (1)					
Strained1	206 (1) 20.0 (2)	+727 (1) ↑ +1101 to +1479 (2)	6.34	147	↑+1302 to +1718 +476	24.2
	↓ +1553 to +1487 (2), +489 (1)					
Strained2	158 (1) 8.90 (2)	+559 (1) ↑+1159 to +1467 (2) +989 (2), +487 (1)	3.83	182	↑ +960 to +1192 +496	15.9
Near rupture	Not applicable			409 (1) 13.0 (2)	+931 (1) ↑+1193 to +1439 (2) +499	4.72

so clear concerning non ferrous metallic alloys[10-12].

Concerning the passive state, which must be artificially obtained by applying a high potential, there are also differences, first between the two types of steel: passivation in two times for the ferrito-pearlitic one, with two partial anodic peaks, the first one (ferrite) corresponding to the unique one of the ferritic steel. About the easiness for reaching the passive state, which can be estimated by the passivation potential and by the critical passivation current, clear deductions are not really possible since the two parameters indicate opposite conclusions. However it can be said that the amount of strain deformation greatly influences the polarization curves, at least their potential-increasing part.

CONCLUSIONS

The active behaviour in corrosion of not alloyed steels when immersed in sulphuric acid solution, and maybe their passive behaviour too, depends on both the plastic strained amount and the orientation. Such dependence may lead to accelerated corrosion in some zones of a steel piece previously subjected to inhomogeneous deformation (as for a piece with varying sections along its axis and plastically deformed in traction), between a not plastically strained zone (great sections with only elastic deformation) and more plastically strained other zones, as well as differently oriented areas. Furthermore the heterogeneous corrosion can also be enhanced by galvanic coupling between such different locations. This can finally result in a local rupture which can be not really anticipated if electrochemical characterization of corrosion rate are not performed on the more sensible zone of the piece.

ACKNOWLEDGEMENTS

The author thanks Sullivan De Sousa and Jean-Pierre Philippe for their participations to the mechanical tensile tests.

REFERENCES

[1] Y.D.Koryagin, N.T.Kareva, M.A.Smirnov; Physics of Metals and Metallography, **55(4)**, 187 **(1983)**.
[2] V.G.Serebryakov, E.I.Ehstrin; Fizika Metallov I Metallovedenie, **2**, 130 **(1992)**.
[3] E.L.Svistunova, A.A.Gulyaev, A.B.Oralbaev; Fizika Metallov I Metallovedenie, **78(1)**, 108 **(1994)**.
[4] J.Zdunek, P.Widlicki, H.Garbacz, J.Mizera, K.J.Kurzydlowski; Diffusion and Defect Data Pt.B: Solid State Phenomena, **114**, 171 **(2006)**.
[5] A.V.Korzinkov, Y.V.Ivanisenko, D.V.Laptionok, I.M.Safarov, V.P.Pilyugin, R.Z.Valiev; Nanostructured Materials, **4(2)**, 159 **(1994)**.
[6] A.Ben Bachir, H.Triche; Mémoire Scientifique Revue de Métallurgie, **71(1)**, 9 **(1974)**.
[7] M.Saled, L.Aries, H.Triche; Mémoire Scientifique Revue de Métallurgie, **71(10)**, 621 **(1974)**.
[8] M.S.Khoma; Fiziko-Khimicheskaya Mekhanika Materialov, **30(1)**, 125 **(1994)**.
[9] X.C.Li, R.L.Eadie, J.L.Luo, Corrosion Engineering Science and Technology, **43(4)**, 297 **(2008)**.
[10] P.Berthod; Materials Science: An Indian Journal, **5(3)**, 161 **(2009)**.
[11] E.Akiyama, Z.Zhang, Y.Watanabe, K.Tsuzaki; Journal of Solid State Electrochemistry, **13(2)**, 277 **(2009)**.
[12] W.Y.Guo, J.Sun, J.S.Wu; Materials Characterization, **60(3)**, 173 **(2009)**.